


Nondegenerate bound-state solitons in multicomponent Bose-Einstein condensatesYan-Hong Qin,^{1,2} Li-Chen Zhao ,^{1,2,*} and Liming Ling^{3,†}¹*School of Physics, Northwest University, Xi'an 710127, China*²*Shaanxi Key Laboratory for Theoretical Physics Frontiers, Xi'an 710127, China*³*School of Mathematics, South China University of Technology, Guangzhou 510640, China*

(Received 15 April 2019; revised manuscript received 23 July 2019; published 15 August 2019)

We investigate nondegenerate bound-state solitons systematically in multicomponent Bose-Einstein condensates, through developing the Darboux transformation method to derive exact soliton solutions analytically. In particular, we show that bright solitons with nodes correspond to the excited bound states in effective quantum wells, in sharp contrast to the bright solitons and dark solitons reported before (which usually correspond to ground state and free state, respectively). We further demonstrate that bound-state solitons with nodes are induced by incoherent superposition of solitons in different components. Moreover, we reveal that the interactions between these bound-state solitons are usually inelastic, caused by the incoherent interactions between solitons in different components and the coherent interactions between solitons in the same component. Additionally, the detailed spectral stability analysis demonstrates the stability of nondegenerate bound-state solitons. The bound-state solitons can be used to study many different physical problems, such as beating dynamics, spin-orbit coupling effects, quantum fluctuations, and even quantum entanglement states.

DOI: [10.1103/PhysRevE.100.022212](https://doi.org/10.1103/PhysRevE.100.022212)**I. INTRODUCTION**

Multicomponent Bose-Einstein condensates (BECs) provide a good platform to study the dynamics of vector solitons [1]. Many different vector solitons have been obtained in two-component BECs, such as bright-bright solitons [2–4], bright-dark solitons [5], dark-antidark solitons [6], dark-dark solitons [7,8], and dark-bright solitons [9,10]. Those soliton states can be related with eigenstates in quantum wells [11]. From the general properties of eigenstates in one-dimensional quantum wells [12], one can know that fundamental bright solitons and dark solitons correspond to the ground state and the first-excited state, respectively, in an effective quantum well. Therefore, bright-bright solitons and dark-dark solitons are degenerate solitons (more than one component admits the same spatial mode), and bright-dark solitons and dark-bright solitons are nondegenerate soliton states. A bright soliton is a bound state which admits zero density at infinity. A dark soliton is a free state which admits nonzero density at infinity. This means that the nondegenerate solitons (dark-bright solitons and bright-dark solitons) both involve a free state [5,9,10]. We would like to look for nondegenerate bound-state solitons (NDBSSs), for which all eigenstates are bound states. The bound-state solitons can be used to investigate much more abundant beating and tunneling dynamics in multicomponent BECs [13]. Many other different physical problems, such as spin-orbit coupling effects [14–17], quantum fluctuations [18–23], and even quantum entanglement states [24], can be investigated.

In this paper, we obtain NDBSSs in multicomponent BECs with attractive interactions, by performing a Darboux transformation. Especially, we note that bright solitons with nodes correspond to the excited eigenstates in the effective quantum wells. The incoherent superposition between solitons in different components can be used to understand the formation of NDBSSs. The incoherent interaction corresponds to the nonlinear interaction between solitons in different components, for which the relative phase of solitons does not affect the interaction patterns. Furthermore, we investigate the interference properties of the NDBSSs. We show that the interference between them exhibits multiperiodicity, significantly differing from scalar solitons or bright-dark solitons. Moreover, our analysis reveals that the interactions between NDBSSs are inelastic in general, induced by the nonlinear incoherent interactions between solitons in different components and the nonlinear coherent interactions between solitons in same component. Double-hump and triple-hump solitons are presented in two-component and three-component BECs, respectively. We also show that NDBSSs admit spectral stability. These fascinating dynamics of NDBSSs enrich the nonlinear dynamics in BECs greatly. Similar studies can be extended to cases with more than three components, and more abundant bound-state solitons are expected.

Our presentation is structured as follows. In Sec. II, we introduce the theoretical model and present the NDBSSs solutions. We further show that the incoherent interactions between solitons in different components can be used to understand the formation of these bound-state solitons. In Sec. III, we reveal that the collisions of NDBSSs are usually inelastic, due to the incoherent interactions and the coherent interactions between these bound-state solitons. In Sec. IV, we exhibit the NDBSSs in three-component BECs. In Sec. V, the stability of NDBSSs is discussed in detail. Possibilities

*zhaolichen3@nwu.edu.cn

†linglm@scut.edu.cn

to observe them are discussed in BEC systems. Finally, we summarize our results in Sec. VI.

II. THEORETICAL MODEL AND NONDEGENERATE BOUND-STATE SOLITON SOLUTIONS

In the framework of the mean-field theory, the dynamics of two-component BECs can be described well by the following dimensionless two-component coupled nonlinear Schrödinger equations [25]:

$$\begin{aligned} iq_{1,t} + q_{1,xx} + 2(|q_1|^2 + |q_2|^2)q_1 &= 0, \\ iq_{2,t} + q_{2,xx} + 2(|q_1|^2 + |q_2|^2)q_2 &= 0, \end{aligned} \quad (1)$$

where $q_1(x, t)$ and $q_2(x, t)$ represent the mean-field wave functions of the two-component BECs [26]. The interactions between atoms are attractive for the above model, and similar discussions can be had for repulsive interactions cases. The model can be also used to describe the evolution of light in nonlinear optical fibers [27,28]. With the aid of the Darboux transformation (DT) [29–32], the Hirota method [33,34], the Bäcklund transformation [35], and the Kakomtsev-Petviashvili hierarchy reduction method [36–38], many different vector solitons have been obtained in various nonlinear systems, such as bright-bright solitons [2,39,40], bright-dark solitons [5], dark-dark solitons [7,8], and dark-bright solitons [9,10,35]. We would like to look for NDBSSs, for which all eigenstates are bound states, in contrast to the reported bright-dark soliton [5] and the dark-bright soliton [9,10,35].

DT is a very powerful method for constructing soliton solutions. Therefore, we would like to develop a DT method to derive the NDBSSs. The twofold DT with spectral parameters $\lambda_1 = a_1 + ib_1$ and $\lambda_2 = a_1 + ib_2$ generates one NDBSS. The derivation process is given in Appendix A in detail, which is different from the processes for generating bright-bright solitons and bright-dark solitons [29–32]. The exact general double-hump soliton solution for Eq. (1) can be written as follows:

$$\begin{aligned} q_1(x, t) &= -2ib_1c_{11}^* \frac{N_1}{M_1} e^{-i[a_1x + (a_1^2 - b_1^2)t]}, \\ q_2(x, t) &= -2ib_2c_{22}^* \frac{N_2}{M_1} e^{-i[a_1x + (a_1^2 - b_2^2)t]}. \end{aligned} \quad (2)$$

with

$$\begin{aligned} N_1 &= \left(\frac{b_1 - b_2}{b_1 + b_2} + |c_{22}|^2 e^{-2b_2(x+2a_1t)} \right) e^{-b_1(x+2a_1t)}, \\ N_2 &= \left(\frac{b_2 - b_1}{b_1 + b_2} + |c_{11}|^2 e^{-2b_1(x+2a_1t)} \right) e^{-b_2(x+2a_1t)}, \\ M_1 &= |c_{11}|^2 e^{-2b_1(x+2a_1t)} + |c_{22}|^2 e^{-2b_2(x+2a_1t)} \\ &\quad + |c_{11}c_{22}|^2 e^{-2(b_1+b_2)(x+2a_1t)} + \frac{(b_1 - b_2)^2}{(b_1 + b_2)^2}, \end{aligned}$$

where a_1 , b_1 , and b_2 are real parameters, and c_{11} and c_{22} are complex parameters. The velocity of the soliton is $-2a_1$. The parameters b_1 , b_2 , $|c_{11}|$, and $|c_{22}|$ determine the soliton profile. According to the expressions in Eq. (2), we see that soliton profiles will be kept except for the translation of the position under the transforms $|c_{11}| \rightarrow |c_{11}|e^{b_1\delta}$ and $|c_{22}| \rightarrow |c_{22}|e^{b_2\delta}$,

where δ is an arbitrary real constant. These parameters non-trivially contribute to the profile of the soliton. It is noted that the solitons in two components admit different modes. When $b_1 < b_2$, the soliton in the q_2 component admits no node, and the one in the q_1 component always has one node, and vice versa. Since a nonlinear Schrödinger equation can be mapped to a linear Schrödinger equation with proper quantum wells [11,12], the nonlinear term $-2|q_1(x, t)|^2 - 2|q_2(x, t)|^2$ in Eq. (1) can be understood as an effective quantum well, $V(x, t)$. If $-2|q_1(x, t)|^2 - 2|q_2(x, t)|^2$ does not depend on time, the soliton states can be related with eigenproblems in the quantum well $V(x)$, namely, $[-\partial_x^2 + V(x)]q_j = \mu_j q_j$. Then the soliton solutions can be mapped to the eigenvalues μ_j and the eigenstates q_j in the effective quantum well. From the node properties of the corresponding eigenstates in quantum wells [12], we know that the eigenstate with one node corresponds to the first-excited state in effective quantum wells [11]. Therefore, the bound-state solitons in two components correspond to ground state and first-excited state in effective quantum wells respectively. A bound-state soliton with one node is in sharp contrast to the bright soliton and the dark soliton reported before. The NDBSSs are similar to the ‘‘soliton complexes’’ which have been used to describe different composition solitons [41–43]; however, it is not convenient to distinguish nodes of solitons based on the concept of ‘‘soliton complexes.’’ To emphasize the node properties and their relations with eigenstates in quantum wells, we discuss them from the quantum well viewpoint. Moreover, the Manakov model can be transformed into the parametrically driven nonlinear Schrödinger equation [42,43], when the solutions can be transformed into stationary states of the Manakov model. In this way, NDBSSs can be related with the soliton complexes in Refs. [42,43]. Additionally, for the soliton solutions which cannot be transformed into stationary states of the Manakov model, they do not hold anymore for the parametrically driven nonlinear Schrödinger equation. In what follows, we discuss the profile types of the fundamental NDBSSs.

The profiles of NDBSSs can be mainly classified as three different types: asymmetric double-hump solitons (two components both admit asymmetric double-hump solitons), symmetric single-hump–double-hump solitons (one component admits single-hump solitons and the other component has a symmetric double-hump soliton), and symmetric double-hump solitons (two components both admit symmetric double-hump solitons). This classification is different from the one given in Ref. [44], based on different aspects of soliton profiles. The three different cases are shown in Figs. 1(a1)–1(a3); the solid blue line and the dashed red line corresponds to the q_1 component and the q_2 component, respectively. Figure. 1(a1) depicts the intensity profiles of asymmetric double-hump solitons in both components. The solitons in the q_1 component and the q_2 component correspond to the first-excited state and the ground state, respectively, in an effective quantum double-well potential. Particularly, we find that the asymmetric double-hump soliton solution, Eq. (2), can be reduced to a symmetric form by choosing the parameters $c_{11} = c_{22} = \sqrt{3}/3$, $b_2 = 2b_1$, and $\delta = 0$. For this case, we rewrite the solutions as $q_1 = \sqrt{3}b_1 \operatorname{sech}[b_1(x + 2a_1t)] \tanh[b_1(x + 2a_1t)] e^{-i[a_1x + (a_1^2 - b_1^2)t - \pi/2]}$ and $q_2 = \sqrt{3}b_1$

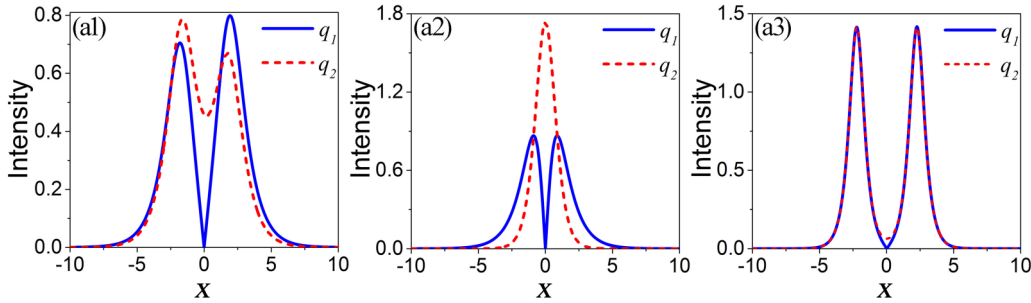


FIG. 1. Three different density profiles for double-hump solitons in two-component coupled systems: (a1) asymmetric double-hump solitons in both components, (a2) symmetric single-hump–double-hump solitons, and (a3) approximate symmetric double-hump solitons in both components. solid blue line and the dashed red line correspond to the q_1 component and the q_2 component, respectively. It is seen that solitons in q_1 and q_2 components correspond to first-excited state and ground state, respectively, in the effective double-well potential. The parameters are as follows: (a1) $c_{11} = c_{22} = 1$, $a_1 = 0$, $b_1 = 1$, $b_2 = 1.1$, and $\delta = -2.8$; (a2) $c_{11} = c_{22} = \sqrt{3}/3$, $a_1 = 0$, $b_1 = 1$, $b_2 = 2b_1$, and $\delta = 0$; and (a3) $c_{11} = c_{22} = 1$, $a_1 = 0$, $b_1 = 2$, $b_2 = 2.001$, and $\delta = -4.1$.

$\text{sech}^2[b_1(x + 2a_1t)]e^{-i[a_1x + (a_1^2 - 4b_1^2)t + \pi/2]}$. The amplitudes of the q_1 and q_2 components are $\sqrt{3}b_1/2$ and $\sqrt{3}b_1$, respectively. One can see that a symmetric double-hump bright soliton presents in the q_1 component, which corresponds to the first-excited bound state, while a single-hump ground bound-state soliton emerges in the q_2 component. This type of soliton can be seen as a symmetric single-hump–double-hump soliton. As an example, we show it in Fig. 1(a2). Additionally, when b_1 and b_2 are very close to each other, Eq. (2) will show nearly symmetrical double-hump bright solitons in both components. Typical intensity profiles are shown in Fig. 1(a3). The two humps distribute symmetrically in each component for this case. Remarkably, it is clear that a bright soliton with one node (the first-excited bound-state soliton) emerges in just one of the components for all three cases.

The soliton solutions of the above Manakov model have been studied widely. However, bright solitons with nodes are absent in most of the previously published studies on vector solitons [29–32]. Therefore, we would like to discuss why there are NDBSSs in the coupled systems. Based on the derivation method for NDBSSs, we note that these bound-state solitons are generated from two solitons with zero relative velocity and some special parameters. The analysis indicates that the choice of special parameters corresponds to the incoherent interactions between solitons in different components. The incoherent interaction corresponds to the nonlinear interaction between incoherent solitons, for which the relative phase of solitons does not affect the interaction pattern. It is different from the coherent interaction of two solitons in the same component for which the relative phase of them affects the interaction pattern. The double-hump soliton is related to two incoherent solitons, for which each bright soliton emerges in just one certain component (they are phase separated), in contrast to the well-known bright-bright soliton. Therefore, we investigate the interaction of two incoherent solitons with different velocities, to investigate the role of relative velocity in forming the NDBSSs. This can be done exactly by changing the spectral parameters $\lambda_1 = a_1 + ib_1$ and $\lambda_2 = a_2 + ib_2$ in the solution Eq. (A5). We change the velocity of the soliton ($v_j = -2a_j$) in each component, and other parameters are fixed as in Fig. 1(a1). The relevant dy-

namical processes of incoherent interactions between solitons are depicted in Fig. 2, and the relative velocities of solitons ($v_2 - v_1$) in two components correspond to 0.08, 0.004, and 0.0004 from top to bottom, respectively (see captions for detailed parameter settings). The characters of incoherent interactions between solitons are shown clearly in Fig. 2(a). The incoherent interaction mainly includes two cases: incoherent collision and incoherent superposition. Incoherent superposition can be approached from incoherent collision by decreasing the relative velocity. One can see that the relative velocity between solitons is smaller, and the nonlinear

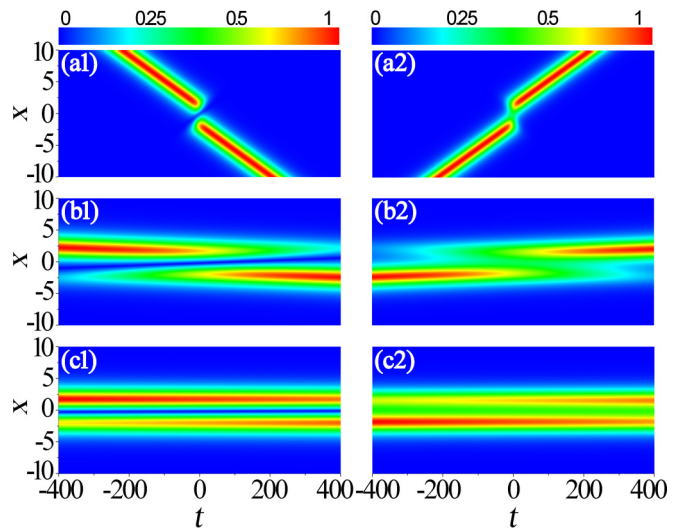


FIG. 2. The incoherent interactions between solitons in different components with different relative velocities ($2a_1 - 2a_2$). From top to bottom, the parameters are as follows: (a1) and (a2) $a_1 = -a_2 = 0.02$, (b1) and (b2) $a_1 = -a_2 = 0.001$, and (c1) and (c2) $a_1 = -a_2 = 0.0001$. The left panels show the density distributions of the q_1 component; the right panels show the density distributions of the q_2 component. The evolution dynamics suggest that nondegenerate bound-state solitons are induced by incoherent superpositions of bright solitons in different components. The other parameters are $c_{11} = c_{22} = 1$, $b_1 = 1$, $b_2 = 1.1$, and $\delta = -2.8$ [the same as those in Fig. 1(a1)].

incoherent interaction between solitons in different components is becoming stronger. When the relative velocity of solitons decreases to zero, the nonlinear incoherent interaction will become an incoherent superposition of them, which induces the profile of the bright soliton in one of component changes to be a double-hump soliton with one node (first-excited bound eigenstate) and the profile of the bright soliton in the other component becomes a double-hump soliton with no node (ground bound state), such as solitons in Fig. 1(a1). These dynamical processes indicate that NDBSSs are induced by the incoherent superposition between solitons in different components.

It should be mentioned that similar multihump solitons have been observed for a long time in dispersive nonlinear medium [45–47]. Stationary multihump solitons have also been obtained in Kerr-like media [48]. Recently, many different static nondegenerate solitons were derived from eigenstates in some certain quantum wells [11]. However, bright solitons with nodes are symbiotic with dark solitons; that is, the bound state and the free state always coexist in the coupled systems. Moreover, these solutions are stationary and it is inconvenient to discuss their collision properties analytically. Very recently, nondegenerate solitons in the Manakov system were reported by the Hirota’s bilinear method [44]. In this paper, we develop the DT method to derive NDBSSs, which enables us to discuss the underlying mechanism for these bound-state solitons. Furthermore, we develop the DT method to investigate the collision processes between the NDBSSs analytically.

III. COLLISION BETWEEN DIFFERENT NONDEGENERATED SOLITONS

First, we investigate the collision between one NDBSS and one degenerate bright soliton, by performing the threefold DT with spectral parameters $\lambda_1 = a_1 + ib_1$, $\lambda_2 = a_1 + ib_2$, and $\lambda_3 = a_2 + ib_3$ (see Appendix A for the solution process). More complicated interactions between solitons can be investigated by performing the N -fold DT in Appendix A, Eq. (A8). For this case, typical densities are depicted in the Figs. 3(a1) and 3(a2) corresponding to the q_1 component and the q_2 component, respectively. It is seen that the interference patterns between an asymmetric double-hump soliton and a single-hump soliton appear in both components. One first-excited-state soliton interferes with a ground-state soliton in the q_1 component, while two ground-state solitons collide with each other in the q_2 component. Detailed analysis indicates that the collisions between them are usually inelastic, and they can be elastic under some special initial conditions.

Second, we investigate the interaction between two NDBSSs by performing the fourfold DT with spectral parameters $\lambda_1 = a_1 + ib_1$, $\lambda_2 = a_1 + ib_2$ (generates one NDBSS), $\lambda_3 = a_2 + ib_3$, and $\lambda_4 = a_2 + ib_4$ (generates another NDBSS). We exhibit the dynamical evolution of them in the right-hand panels of Fig. 3, based on the two double-hump solitons solution Eq. (A7). Figures 3(b1) and 3(b2) correspond to the q_1 component and the q_2 component, respectively. As one can see in Figs. 3(b1) and 3(b2), the collision of two identical symmetric double-hump solitons (two first-excited bound-state solitons) in the q_1 component and two identical single-hump solitons

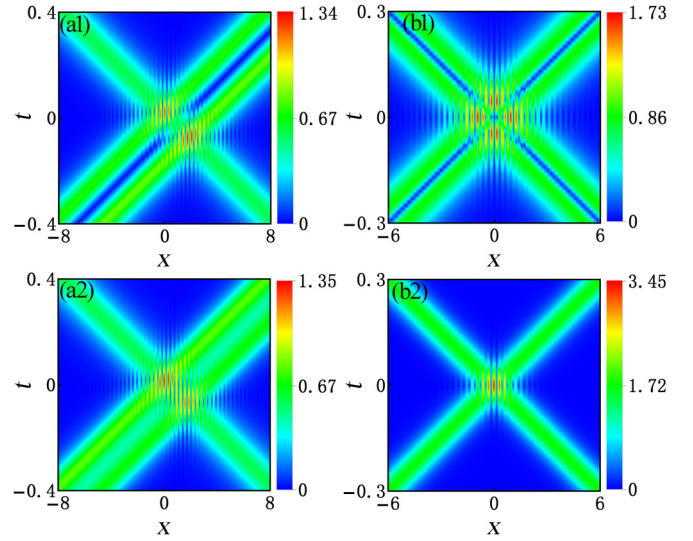


FIG. 3. The collision dynamics between one nondegenerate bound-state soliton and one degenerate bright soliton or one nondegenerate bound-state soliton. (a1) and (a2): The interference behavior between an asymmetric double-hump soliton (moving to the right direction) and a degenerate bright soliton (moving to the left direction). Related parameters are $c_{21} = c_{12} = 0$, $c_{11} = c_{22} = c_{13} = c_{23} = 1$, $a_1 = -10$, $a_2 = 10$, $b_1 = 1$, $b_2 = 1.1$, $b_3 = 0.8$, and $\delta_1 = \delta_2 = 0$. (b1) and (b2): The interference patterns between two nondegenerate bound-state solitons. The parameters are $c_{11} = c_{22} = c_{13} = c_{24} = \sqrt{3}/3$, $a_1 = 10$, $a_2 = -10$, $b_1 = 1$, $b_2 = 2$, $b_3 = 1$, $b_4 = 2$, and $\delta_1 = \delta_2 = 0$. The top panels show the density of the first component, and the bottom panels show the density of the second component. The soliton profiles change too slightly to be visible after the collision at these parameters.

(two ground bound-state solitons) in the q_2 component both generate interference patterns. Moreover, we further explore the interference properties of them by the asymptotic analysis technique (see the detailed solution process in Appendix A). Interestingly, we find that the interference of double-hump solitons presents multiperiodicity. The periodic functions are governed by the factors $\sin[(a_1 - a_2)x + (a_1^2 - a_2^2 + b_3^2 - b_1^2)t]$ and $\sin[(a_1 - a_2)x + (a_1^2 - a_2^2 - b_2^2 + b_4^2)t]$ and their corresponding cosine forms. These mean that there are three periodic oscillation behaviors in the interference process of two double-hump bright solitons. The spatial period is $D = 2\pi/(a_1 - a_2) = 4\pi/(v_1 - v_2)$, and the temporal periods are $T_1 = 2\pi/(a_1^2 - a_2^2 + b_3^2 - b_1^2)$ and $T_2 = 2\pi/(a_1^2 - a_2^2 - b_2^2 + b_4^2)$, in a striking contrast to interference patterns between bright solitons reported before [49]. This comes from more than two energy eigenvalues involved in the interference processes. In Figs. 3(b1) and 3(b2), only the spatial interference pattern is visible, due to the parameters settings $a_1^2 = a_2^2$, $b_1 = b_3$, and $b_2 = b_4$, which make two temporal periods be zero. For Figs. 3(a1) and 3(a2), the parameter settings make two temporal periods too small to be visible (see caption for details).

It should be emphasized that the collision dynamics between bound-state solitons in Fig. 3 are indeed inelastic, where the solitons’ profiles change too slightly to be visible after the collision. Further analysis suggests that the collisions

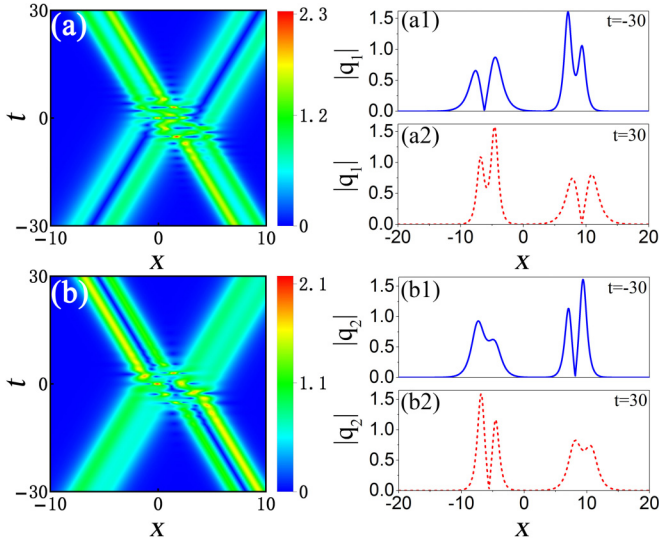


FIG. 4. The inelastic collision between two nondegenerate bound-state solitons. Left panels: Dynamical evolution for coherent collision of nondegenerate bound-state solitons. Right panels: Intensity plots for both components before ($t = -30$, solid blue line) and after ($t = 30$, dashed red line) the collision. It is seen that profiles of double-hump solitons indeed change after the collision. The analysis suggests that the collisions between these bound-state solitons are usually inelastic, due to the incoherent interaction and the coherent collision between them. The parameters are $c_{11} = c_{22} = c_{13} = c_{24} = 1$, $a_1 = -1/10$, $a_2 = 1/10$, $b_1 = 1$, $b_2 = 1.2$, $b_3 = 2$, $b_4 = 1.9$, and $\delta_1 = \delta_2 = 0$.

between bound-state solitons are usually inelastic unless the parameters satisfy the sufficient condition Eq. (A15). Inelastic collision refers to that the soliton's profile changes after the collision. A typical example for inelastic collision is shown in Fig. 4, where two double-hump solitons collide with each other in both components. The panels on the left show the related density evolutions; Figs. 4(a) and 4(b) correspond to the q_1 component and the q_2 component, respectively. The panels on the right depict the corresponding intensity profiles of two solitons before ($t = -30$, solid blue line) and after ($t = 30$, dashed red line) the collision in both components. These figures clearly show that the double-hump solitons' profiles undergo dramatic change after the collision in each component [see Figs. 4(a1) and 4(a2) and Figs. 4(b1) and 4(b2)]. Then, what causes inelastic collisions of NDBSSs? As mentioned in Sec. II, NDBSSs are induced by the incoherent interactions between solitons in different components. Moreover, the collision between NDBSSs also involve the coherent collision between solitons in the same component. Therefore, the incoherent interactions between solitons in different components and the coherent collision between solitons in the same component both affect collision properties. By investigating the interactions between solitons with different ϵ values (the spectral parameters are chosen as $\lambda_1 = a_1 + ib_1$, $\lambda_2 = a_1 + \epsilon_1 + ib_2$, $\lambda_3 = a_2 + ib_3$, and $\lambda_4 = a_2 + \epsilon_2 + ib_4$), we can see that the collisions between bound-state solitons are usually inelastic.

Very recently, three-component soliton states were observed in a spinor BEC system [50]. Motivated by these devel-

opments, we would like to extend our studies on NDBSSs to three-component BECs. Similar discussions can be extended to cases with more than three components.

IV. NONDEGENERATE BOUND-STATE SOLITONS IN THREE-COMPONENT CONDENSATES

In this section, we consider the NDBSSs in three-component BECs with attractive interactions. The dynamics can be described well by the following three-component, coupled nonlinear Schrödinger equations in dimensionless form ($j = 1, 2, 3$):

$$iq_{j,t} + q_{j,xx} + 2(|q_1|^2 + |q_2|^2 + |q_3|^2)q_j = 0. \quad (3)$$

By directly performing the similar DT method with $\lambda_1 = a_1 + ib_1$, $\lambda_2 = a_1 + ib_2$, and $\lambda_3 = a_1 + ib_3$ as presented in Appendix A, the exact triple-hump bound-state soliton solution of Eq. (3) can be written as follows (we do not show the explicit solution process here for brevity):

$$\begin{aligned} q_1(x, t) &= -2ib_1c_1e^{-i\alpha_1} \left(\frac{\chi_1}{\Xi_1} + \frac{2b_3\Delta_1\Delta_2}{(b_2 + b_3)^2\Xi_2\Xi_1^2}e^{\beta_1} \right), \\ q_2(x, t) &= -2ib_2c_2e^{-i\alpha_2} \left(\frac{\chi_2}{\Xi_1} + \frac{2b_3\Delta_1\Delta_3}{(b_2 + b_3)^2\Xi_2\Xi_1^2}e^{\beta_2} \right), \\ q_3(x, t) &= -2ib_3c_3 \frac{\Delta_1e^{-i\alpha_3+\beta_3}}{(b_2 + b_3)\Xi_2\Xi_1}, \end{aligned} \quad (4)$$

where $\beta_j = -b_j(x + 2a_1t)$ and $\alpha_j = a_1x + (a_1^2 - b_j^2)t$. The explicit expressions of $\Xi_{1,2}$, $\chi_{1,2}$, and $\Delta_{1,2,3}$ are given in Appendix B. a_1 , b_1 , b_2 , and b_3 are real parameters; c_1 , c_2 , and c_3 are complex parameters. The velocity of the soliton is $-2a_1$. Parameters b_1 , b_2 , b_3 , $|c_1|$, $|c_2|$, and $|c_3|$ govern the soliton profiles. According to the expressions in Eq. (4), we see that the profiles of solitons will be kept except for the translation of position under the transforms $|c_1| \rightarrow |c_1|e^{b_1\delta}$, $|c_2| \rightarrow |c_2|e^{b_2\delta}$, and $|c_3| \rightarrow |c_3|e^{b_3\delta}$, where δ is an arbitrary real constant. These parameters nontrivially contribute to the profiles of solitons. A typical example of the intensity profiles are displayed in Fig. 5. It can be seen that a triple-hump bright soliton is exhibited in each component. The effective quantum wells for this three-component case is $-2|q_1(x, t)|^2 - 2|q_2(x, t)|^2 - 2|q_3(x, t)|^2$, and it is a triple-well form. Based on the correspondence between solitons and eigenstates in quantum wells [11,12], one can know that the triple-hump bright soliton with no node in the q_3 component is the ground bound state (dashed green line in Fig. 5), the triple-hump bright soliton with one node in the q_2 component is the first-excited bound state (dotted-dashed blue line in Fig. 5), and the triple-hump bright soliton with two nodes in the q_1 component is the second-excited bound state (solid red line in Fig. 5) in the effective quantum wells. Double-hump or single-hump solitons can be also obtained in the three-component case by choosing some proper parameters. This suggests that more abundant NDBSSs exist in multi-component coupled systems, since many-component coupled BECs can induce deeper quantum wells [11]. Similarly, the collision between triple-hump solitons and single-hump solitons can be investigated in three-component BECs by performing the fourfold DT. The interaction between triple-hump solitons and double-hump

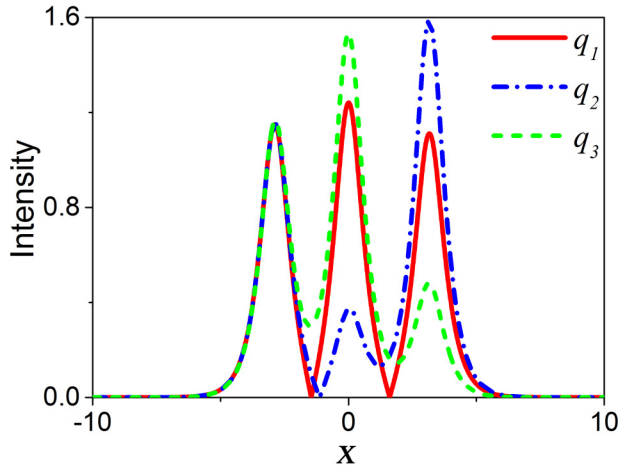


FIG. 5. Intensity profiles for triple-hump bright solitons of three-component BECs. The triple-hump bright soliton with no node in the q_3 component is the ground bound state (dashed green line), the triple-hump bright soliton with one node in the q_2 component is the first-excited bound state (dotted-dashed blue line), and the triple-hump bright soliton with two nodes in the q_1 component is the second-excited bound state (solid red line) in the effective quantum wells. The parameters are $c_1 = c_2 = c_3 = 1$, $a_1 = 0$, $b_1 = 1.99$, $b_2 = 2$, $b_3 = 2.02$, and $\delta = -5.2$.

solitons can be studied by performing the fivefold DT. The interplay between two triple-hump solitons can be explored by performing the sixfold DT. The inelastic collision of these bound-state solitons can be also expected.

V. STABILITY OF NONDEGENERATE BOUND-STATE SOLITONS

We discuss the stability of these bound-state solitons by calculating the Bogoliubov-de Gennes excitation spectrum around a stationary soliton solution. We introduce the ansatz $\mathbf{q} = \mathbf{q}_0 + \epsilon[\mathbf{P}e^{-i\lambda t} + \mathbf{Q}^*e^{i\lambda^*t}]e^{-i\mu t}$, where \mathbf{q}_0 is a NDBSS solution, ϵ is a small parameter, and $\{\lambda, (\mathbf{P}, \mathbf{Q}^*)\}$ defines an eigenvalue-eigenvector pair. Then, substituting this ansatz into related dynamical equations and linearizing the equations, we arrive at $O(\epsilon)$ at an eigenvalue problem for eigenvectors $(\mathbf{P}, \mathbf{Q}^*)$ and eigenvalues λ . Note that the latter may, in principle, be complex, i.e., $\lambda = \lambda_r + i\lambda_i$, instability corresponds to $\lambda_i \neq 0$. As an example, we consider the case of the asymmetric double-hump solitons in both components based on the solution Eq. (2). The corresponding eigenvalue spectrum is shown in Fig. 6, and the parameters are the same as those in Fig. 1(a). It can be seen that the spectrum of the double-hump solitons consists of purely real eigenvalues, showing spectral stability. Numerical simulations from the corresponding initial conditions also support the stability of solitons. On the other hand, experimental observations demonstrated that two-component solitons can be produced based on well-developed density and phase modulation techniques [9,51,52]. Solitons' interactions have also been demonstrated experimentally in BEC systems [53–56]. Therefore, based on the established experimental techniques,

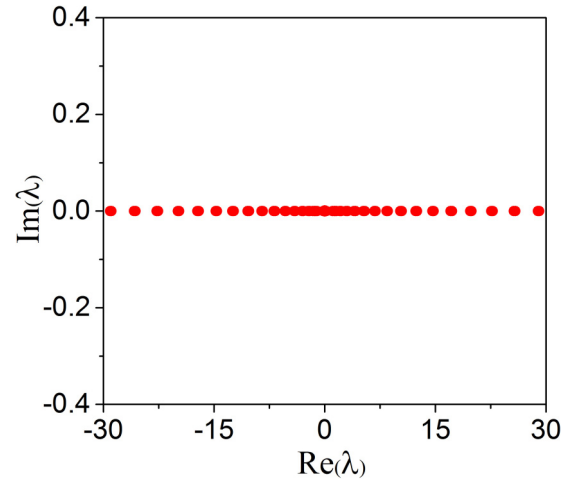


FIG. 6. The excitation spectrum of nondegenerate bound-state solitons. It is seen that nondegenerate bound-state solitons admit spectral stability. The related parameters are same as those in Fig. 1(a).

the presented NDBSSs have many possibilities to be observed in multicomponent attractive BECs.

VI. CONCLUSION AND DISCUSSION

In summary, we derive and investigate double-hump and tripe-hump bound-state solitons in multicomponent BECs. The analysis indicates that bright solitons with nodes correspond to the excited bound eigenstates in the effective quantum wells. Particularly, we reveal that the incoherent superposition between solitons in different components is the generation mechanism of the bound-state solitons. Furthermore, we demonstrate that the collisions of NDBSSs are inelastic in general cases, which are induced by incoherent interactions and coherent collisions. More abundant bound-state solitons are expected in multi-component coupled BECs.

In fact, these NDBSSs can be also obtained from more general multisolitons (obtained using different methods) with some special constraint conditions. But the constraint conditions were not addressed in previous studies [34–36]. Our incoherent superposition form can be used to determine the constraint conditions. Moreover, NDBSSs can be mapped to eigenstates in a quantum well, in sharp contrast to the general multisolitons.

Note added. Recently, we noticed nondegenerate solitons were discussed in nonlinear optical fibers by the Hirota bilinear method [44]. In this paper, we perform the Darboux transformation method to derive NDBSS solutions. Moreover, the discussions on the mechanism and the node properties could be helpful for our understanding of NDBSSs.

ACKNOWLEDGMENTS

This work is supported by the National Natural Science Foundation of China (Contracts No. 11775176 and No. 11771151), the Basic Research Program of Natural Science of Shaanxi Province (Grant No. 2018KJXX-094), the Key Innovative Research Team of Quantum Many-Body Theory and

Quantum Control in Shaanxi Province (Grant No. 2017KCT-12), and the Major Basic Research Program of Natural Science of Shaanxi Province (Grant No. 2017ZDJC-32).

APPENDIX A: DERIVATION OF THE VECTOR DOUBLE-HUMP BRIGHT SOLITON SOLUTIONS OF EQ. (1)

The two-component coupled nonlinear Schrödinger equation, Eq. (1), is the compatibility condition of the linear spectral problems [25,31]:

$$\begin{aligned}\Phi_x &= U(x, t; \lambda)\Phi, \\ \Phi_t &= V(x, t; \lambda)\Phi,\end{aligned}\quad (\text{A1})$$

where

$$U = \begin{pmatrix} -i\frac{2}{3}\lambda & q_1 & q_2 \\ -q_1^* & \frac{i}{3}\lambda & 0 \\ -q_2^* & 0 & \frac{i}{3}\lambda \end{pmatrix},$$

$$V = U\lambda + \begin{pmatrix} i|q_1|^2 + i|q_2|^2 & iq_{1x} & iq_{2x} \\ iq_{1x}^* & -i|q_1|^2 & -iq_2q_1^* \\ iq_{2x}^* & -iq_2^*q_1 & -i|q_2|^2 \end{pmatrix}. \quad (\text{A2})$$

The star denotes the complex conjugate. With the trivial seed solutions $q_1[0] = 0$, $q_2[0] = 0$ and the spectral parameter $\lambda = \lambda_j = a_j + b_j i$ ($j = 1, 2, \dots, N$), the vector eigenfunctions of the linear system Eq. (5) can be written as

$$\Phi_j = \begin{pmatrix} \Phi_{1j} \\ \Phi_{2j} \\ \Phi_{3j} \end{pmatrix} = \begin{pmatrix} e^{-2\theta_j} \\ c_{1j}e^{\theta_j} \\ c_{2j}e^{\theta_j} \end{pmatrix}, \quad \theta_j = \frac{i}{3}\lambda_j x + \frac{i}{3}\lambda_j^2 t, \quad (\text{A3})$$

where c_{1j} and c_{2j} are the coefficients of eigenfunctions, and they are complex parameters. The fundamental bright solitons can be obtained by the following Darboux transformation:

$$\begin{aligned}\Phi[1] &= T[1]\Phi, \quad T[1] = \mathbb{I} - \frac{\lambda_1 - \lambda_1^*}{\lambda - \lambda_1^*} P[1], \\ q_1[1] &= q_1[0] + (\lambda_1^* - \lambda_1)(P[1])_{12}, \\ q_2[1] &= q_2[0] + (\lambda_1^* - \lambda_1)(P[1])_{13}.\end{aligned}\quad (\text{A4})$$

Here, $P[1] = \frac{\Phi_1 \Phi_1^\dagger}{\Phi_1^\dagger \Phi_1}$, where Φ_1 is a special solution at $\lambda = \lambda_1$; a dagger denotes the matrix transpose and complex conjugate. $(P[j])_{ij}$ represents the entry of matrix $P[j]$ in the first row and j column. To obtain a double-hump one soliton, we need to do the second step of the transformation. We employ Φ_2 , which is mapped to $\Phi_2[1] = T[1]|_{\lambda=\lambda_2} \Phi_2$; one double-hump soliton solution can be obtained with the spectral parameter $\lambda_2 = a_1 + ib_2$:

$$\begin{aligned}\Phi[2] &= T[2]\Phi[1], \quad T[2] = \mathbb{I} - \frac{\lambda_2 - \lambda_2^*}{\lambda - \lambda_2^*} P[2], \\ q_1[2] &= q_1[1] + (\lambda_2^* - \lambda_2)(P[2])_{12}, \\ q_2[2] &= q_2[1] + (\lambda_2^* - \lambda_2)(P[2])_{13},\end{aligned}\quad (\text{A5})$$

where $P[2] = \frac{\Phi_2[1]\Phi_2[1]^\dagger}{\Phi_2[1]^\dagger\Phi_2[1]}$. For this case, we choose the coefficients of the eigenfunctions $\Phi_{1,2}$ in Eq. (A3) in the following way: (i) $c_{21} = c_{12} = 0$, and c_{11} and c_{22} are nonzero complex parameters, or (ii) $c_{11} = c_{22} = 0$, and c_{21} and c_{12} are nonzero complex parameters. The corresponding simplified solution

has been present in Eq. (2). Examples of the relevant intensity profiles have been exhibited in Fig. 1.

To study the interaction between nondegenerate solitons, one needs to do a multiple-step transition. For example, by performing the third step of the transition, we employ Φ_3 , which is mapped to $\Phi_3[2] = (T[2]\Phi_3[1])|_{\lambda=\lambda_3}$, with $\Phi_3[1] = (T[1]\Phi_3)|_{\lambda=\lambda_3}$, and then the collision between a double-hump soliton and a single-hump soliton can be obtained with the spectral parameter $\lambda_3 = a_2 + ib_3$:

$$\begin{aligned}\Phi[3] &= T[3]\Phi[2], \quad T[3] = \mathbb{I} - \frac{\lambda_3 - \lambda_3^*}{\lambda - \lambda_3^*} P[3], \\ q_1[3] &= q_1[2] + (\lambda_3^* - \lambda_3)(P[3])_{12}, \\ q_2[3] &= q_2[2] + (\lambda_3^* - \lambda_3)(P[3])_{13},\end{aligned}\quad (\text{A6})$$

where $P[3] = \frac{\Phi_3[2]\Phi_3[2]^\dagger}{\Phi_3[2]^\dagger\Phi_3[2]}$. For this case, we choose the coefficients of the eigenfunctions Φ_3 in Eq. (A3) in the following way: (i) c_{13} and c_{23} are nonzero complex parameters, or (ii) $c_{13} = 0$ or (iii) $c_{23} = 0$, and the coefficients of the eigenfunctions $\Phi_{1,2}$ are the same as those in Eq. (A5). A typical example for this case has been shown in Figs. 3(a1) and 3(a2).

Naturally, by performing the fourth-step of the transformation, one can investigate the interaction between two double-hump solitons. We employ Φ_4 , which is mapped to $\Phi_4[3] = (T[3]\Phi_4[2])|_{\lambda=\lambda_4} = (T[3]T[2]T[1]\Phi_4)|_{\lambda=\lambda_4}$, and then two double-hump solitons' solutions can be obtained as follows with the spectral parameter $\lambda_4 = a_2 + ib_4$:

$$\begin{aligned}q_1[4] &= q_1[3] + (\lambda_4^* - \lambda_4)(P[4])_{12}, \\ q_2[4] &= q_2[3] + (\lambda_4^* - \lambda_4)(P[4])_{13},\end{aligned}\quad (\text{A7})$$

where $P[4] = \frac{\Phi_4[3]\Phi_4[3]^\dagger}{\Phi_4[3]^\dagger\Phi_4[3]}$. For this case, the coefficients of the vector eigenfunctions $\Phi_{3,4}$ are analogous to $\Phi_{1,2}$, i.e., (i) $c_{23} = c_{14} = 0$, and c_{13} and c_{24} are nonzero complex parameters, or (ii) $c_{13} = c_{24} = 0$, and c_{23} and c_{14} are nonzero complex parameters. One typical case has been shown in Figs. 3(b1) and 3(b2).

In general, the N -fold Darboux matrix can be constructed as follows:

$$\begin{aligned}\mathbf{T}_N &= \mathbb{I} - \mathbf{X}_N \mathbf{M}_N^{-1} (\lambda \mathbb{I} - \mathbf{D}_N)^{-1} \mathbf{X}_N^\dagger, \\ \mathbf{X}_N &= [\Phi_1, \Phi_2, \dots, \Phi_N], \\ \mathbf{D}_N &= \text{diag}(\lambda_1^*, \lambda_2^*, \dots, \lambda_N^*), \\ \mathbf{M}_N &= \begin{pmatrix} \Phi_i^\dagger \Phi_j \\ \lambda_j - \lambda_i^* \end{pmatrix}_{1 \leq i, j \leq N},\end{aligned}\quad (\text{A8})$$

and the Bäcklund transformation between old potential functions and new ones can be written as

$$\begin{aligned}q_1[N] &= q_1 + \frac{\det(\mathbf{M}_{N,1})}{\det(\mathbf{M}_N)}, \\ q_2[N] &= q_2 + \frac{\det(\mathbf{M}_{N,2})}{\det(\mathbf{M}_N)},\end{aligned}\quad (\text{A9})$$

where

$$\mathbf{M}_{N,1} = \begin{bmatrix} \mathbf{M}_N & \mathbf{X}_{N,2}^\dagger \\ \mathbf{X}_{N,1} & 0 \end{bmatrix}, \quad \mathbf{M}_{N,2} = \begin{bmatrix} \mathbf{M}_N & \mathbf{X}_{N,3}^\dagger \\ \mathbf{X}_{N,1} & 0 \end{bmatrix}.$$

Here, $\mathbf{X}_{N,i}$ represents the i th row of matrix \mathbf{X}_N .

For the two double-hump solitons, we choose the parameters as the following: $\lambda_1 = a_1 + b_1 i$, $\lambda_2 = a_1 + b_2 i$, $c_{21} = 0$, and $c_{12} = 0$, and c_{11} and c_{22} are nonzero complex parameters, which determine the first double-hump soliton; and $\lambda_3 = a_2 + b_3 i$, $\lambda_4 = a_2 + b_4 i$, $c_{23} = 0$, and $c_{14} = 0$, and c_{13} and c_{24} are nonzero complex parameters, which determine the second double-hump soliton. The oscillator for the two solitons is governed by the factors $\sin[(a_1 - a_2)x + (a_1^2 - a_2^2 + b_3^2 - b_1^2)t]$, $\cos[(a_1 - a_2)x + (a_1^2 - a_2^2 + b_3^2 - b_1^2)t]$, $\sin[(a_1 - a_2)x + (a_1^2 - a_2^2 - b_2^2 + b_4^2)t]$, and $\cos[(a_1 - a_2)x + (a_1^2 - a_2^2 - b_2^2 + b_4^2)t]$. The velocity of the solitons is controlled by $x + 2a_j t = \text{const}$, $j = 1$ and 2 , respectively, i.e., the velocity of the soliton is equal to $-2a_j$. Assume that $b_j > 0$ ($j = 1, 2, 3, 4$) and $a_1 > a_2$, and fix the parameters of the first double-hump soliton $x + 2a_1 t = \text{const}$, then $x + 2a_2 t = x + 2a_1 t + 2(a_2 - a_1)t$. If $t \rightarrow +\infty$, we have $x + 2a_2 t \rightarrow -\infty$. Then we see that

$$\Phi_3 \parallel \begin{pmatrix} e^{-i\lambda_j x - i\lambda_j^2 t} \\ c_{13} \\ 0 \end{pmatrix} \rightarrow \begin{pmatrix} 0 \\ c_{13} \\ 0 \end{pmatrix}$$

and

$$\Phi_4 \parallel \begin{pmatrix} e^{-i\lambda_j x - i\lambda_j^2 t} \\ 0 \\ c_{24} \end{pmatrix} \rightarrow \begin{pmatrix} 0 \\ 0 \\ c_{24} \end{pmatrix}.$$

Since the order of iteration for the Darboux transformation can be exchanged, we rewrite

$$T[1] = \mathbb{I} - \frac{\lambda_3 - \lambda_3^*}{\lambda - \lambda_3^*} \frac{\Phi_3 \Phi_3^\dagger}{\Phi_3^\dagger \Phi_3} \rightarrow \text{diag}\left(1, \frac{\lambda - \lambda_3}{\lambda - \lambda_3^*}, 1\right)$$

along the line of $x - a_1 t = \text{const}$ as $t \rightarrow \infty$. It follows that

$$\Phi_4[1] \parallel T[1]|_{\lambda=\lambda_4} \begin{pmatrix} 0 \\ 0 \\ c_{24} \end{pmatrix} \rightarrow \begin{pmatrix} 0 \\ 0 \\ c_{24} \end{pmatrix},$$

which deduces that

$$T[2] \rightarrow \text{diag}\left(1, 1, \frac{\lambda - \lambda_4}{\lambda - \lambda_4^*}\right).$$

Combining the first and second Darboux matrices, we obtain

$$T[2]T[1] \rightarrow \text{diag}\left(1, \frac{\lambda - \lambda_3}{\lambda - \lambda_3^*}, \frac{\lambda - \lambda_4}{\lambda - \lambda_4^*}\right),$$

which yields that

$$\begin{aligned} \Phi_1[2] &= T[2]T[1]|_{\lambda=\lambda_1} \Phi_1 \rightarrow \Phi_1^{[+]} = \begin{pmatrix} e^{-2\theta_1} \\ c_{11}^{[+]} e^{\theta_1} \\ 0 \end{pmatrix}, \\ \Phi_2[2] &= T[2]T[1]|_{\lambda=\lambda_2} \Phi_2 \rightarrow \Phi_2^{[+]} = \begin{pmatrix} e^{-2\theta_2} \\ 0 \\ c_{22}^{[+]} e^{\theta_2} \end{pmatrix}, \end{aligned} \quad (\text{A10})$$

where $c_{11}^{[+]} = \frac{\lambda_1 - \lambda_3}{\lambda_1 - \lambda_3^*} c_{11}$ and $c_{22}^{[+]} = \frac{\lambda_2 - \lambda_4}{\lambda_2 - \lambda_4^*} c_{22}$.

Thus, when $t \rightarrow +\infty$, the Darboux matrix tends to

$$\begin{aligned} \mathbf{T}_4 &\rightarrow [\mathbb{I} - \mathbf{X}_2^{[+]}(\mathbf{M}_2^{[+]})^{-1}(\lambda\mathbb{I} - \mathbf{D}_2)^{-1}(\mathbf{X}_2^{[+]})^\dagger] \\ &\times \text{diag}\left(1, \frac{\lambda - \lambda_3}{\lambda - \lambda_3^*}, \frac{\lambda - \lambda_4}{\lambda - \lambda_4^*}\right), \end{aligned} \quad (\text{A11})$$

where

$$\mathbf{X}_2^{[+]} = [\Phi_1^{[+]}, \Phi_2^{[+]}, \mathbf{D}_2 = \text{diag}(\lambda_1^*, \lambda_2^*),$$

and

$$\mathbf{M}_2^{[+]} = \begin{bmatrix} \frac{1 + |c_{11}^{[+]}|^2 e^{6\text{Re}(\theta_1)}}{\lambda_1 - \lambda_1^*} & \frac{1}{\lambda_2 - \lambda_1^*} \\ \frac{1}{\lambda_1 - \lambda_2^*} & \frac{1 + |c_{22}^{[+]}|^2 e^{6\text{Re}(\theta_2)}}{\lambda_2 - \lambda_2^*} \end{bmatrix}.$$

From the Darboux matrix Eq. (A11), we obtain that the double-hump soliton approaches

$$\begin{aligned} q_1[4] &\rightarrow q_1(x, t; a_1, b_1, b_2, c_{11}^{[+]}, c_{22}^{[+]}) \\ q_2[4] &\rightarrow q_2(x, t; a_1, b_1, b_2, c_{11}^{[+]}, c_{22}^{[+]}) \end{aligned} \quad (\text{A12})$$

as $t \rightarrow \infty$ along the line $x + 2a_1 t = \text{const}$, where q_1 and q_2 are given in Eqs. (2). In a similar manner, as $t \rightarrow -\infty$, we have

$$\begin{aligned} q_1[4] &\rightarrow q_1(x, t; a_1, b_1, b_2, c_{11}^{[-]}, c_{22}^{[-]}) \\ q_2[4] &\rightarrow q_2(x, t; a_1, b_1, b_2, c_{11}^{[-]}, c_{22}^{[-]}) \end{aligned} \quad (\text{A13})$$

as $t \rightarrow -\infty$ along the line $x + 2a_1 t = \text{const}$, where $c_{11}^{[-]} = \frac{\lambda_1 - \lambda_3^*}{\lambda_1 - \lambda_3} \frac{\lambda_1 - \lambda_4^*}{\lambda_1 - \lambda_4} c_{11}$ and $c_{22}^{[-]} = \frac{\lambda_2 - \lambda_3^*}{\lambda_2 - \lambda_3} \frac{\lambda_2 - \lambda_4^*}{\lambda_2 - \lambda_4} c_{22}$.

Now we consider the asymptotic behavior of the second soliton. Fixing $x + 2a_2 t = \text{const}$, as $t \rightarrow \pm\infty$, and we have the asymptotic expressions

$$\begin{aligned} q_1[4] &\rightarrow q_1(x, t; a_2, b_3, b_4, c_{13}^{[\pm]}, c_{24}^{[\pm]}) \\ q_2[4] &\rightarrow q_2(x, t; a_2, b_3, b_4, c_{13}^{[\pm]}, c_{24}^{[\pm]}) \end{aligned} \quad (\text{A14})$$

where $c_{13}^{[+]} = \frac{\lambda_3 - \lambda_1^*}{\lambda_3 - \lambda_1} \frac{\lambda_3 - \lambda_2^*}{\lambda_3 - \lambda_2} c_{13}$, $c_{24}^{[+]} = \frac{\lambda_4 - \lambda_1^*}{\lambda_4 - \lambda_1} \frac{\lambda_4 - \lambda_2^*}{\lambda_4 - \lambda_2} c_{24}$, $c_{13}^{[-]} = \frac{\lambda_3 - \lambda_1}{\lambda_3 - \lambda_1^*} c_{13}$, and $c_{24}^{[-]} = \frac{\lambda_4 - \lambda_2}{\lambda_4 - \lambda_2^*} c_{24}$.

In the general case, the interaction between two-hump solitons is still inelastic. But under the special case,

$$\begin{aligned} |c_{11}^{[+]}| &= |c_{11}^{[-]}| e^{b_1 \delta_1}, & |c_{22}^{[+]}| &= |c_{22}^{[-]}| e^{b_2 \delta_1}, \\ |c_{13}^{[+]}| &= |c_{13}^{[-]}| e^{b_3 \delta_2}, & |c_{24}^{[+]}| &= |c_{24}^{[-]}| e^{b_4 \delta_2}, \end{aligned} \quad (\text{A15})$$

the interaction is elastic. In other words, this is the sufficient condition, Eq. (A15), of elastic interaction of a two-hump soliton.

APPENDIX B: THE EXPRESSIONS OF $\Xi_{1,2}$, $\chi_{1,2}$, AND $\Delta_{1,2,3}$

The general one triple-hump soliton solution in a three-component NLSE is expressed as Eq. (4), where $\Xi_{1,2}$, $\chi_{1,2}$, and $\Delta_{1,2,3}$ are written as

$$\begin{aligned} \Xi_1 &= \frac{(b_1 - b_2)^2}{(b_1 + b_2)^2} + |c_1|^2 e^{2\beta_1} + |c_2|^2 e^{2\beta_2} + |c_1|^2 |c_2|^2 e^{2(\beta_1 + 2\beta_2)}, \\ \Xi_2 &= \frac{\Delta_1^2}{(b_2 + b_3)^2 \Xi_1^2} + \frac{4b_1^2 |c_1|^2 \Delta_2^2}{(b_2 + b_3)^2 \Xi_1^2} e^{2\beta_1} + \frac{4b_2^2 |c_2|^2 \Delta_3^2}{(b_2 + b_3)^2 \Xi_1^2} e^{2\beta_2} \\ &\quad + |c_3|^2 e^{2\beta_3}, \end{aligned}$$

$$\Delta_1 = (b_2 - b_3) \left[\frac{(b_1 - b_2)^2 (b_1 - b_3)}{(b_1 + b_2)^2 (b_1 + b_3)} - |c_1|^2 e^{2\beta_1} \right] \\ + (b_2 + b_3) \left[\frac{b_3 - b_1}{b_3 + b_1} + |c_1|^2 e^{2\beta_1} \right] |c_2|^2 e^{2\beta_2}, \\ \Delta_2 = \frac{(b_1 - b_2)(b_2 - b_3)}{(b_1 + b_2)(b_1 + b_3)} - \frac{b_2 + b_3}{b_1 + b_3} |c_2|^2 e^{2\beta_2},$$

$$\Delta_3 = \frac{(b_2^2 - b_1^2)(b_1 - b_3)}{(b_1 + b_2)^2 (b_1 + b_3)} - |c_1|^2 e^{2\beta_1}, \\ \chi_1 = \left[\frac{b_1^2 - b_2^2}{(b_1 + b_2)^2} + |c_2|^2 e^{2\beta_2} \right] e^{\beta_1}, \\ \chi_2 = \left[\frac{b_2^2 - b_1^2}{(b_1 + b_2)^2} + |c_1|^2 e^{2\beta_1} \right] e^{\beta_2}.$$

-
- [1] P. G. Kevrekidis, D. J. Frantzeskakis, and R. Carretero-Gonzalez, *Emergent Nonlinear Phenomena in Bose-Einstein Condensates: Theory and Experiment* (Springer, Berlin, 2008).
- [2] X. F. Zhang, X. H. Hu, X.-X. Liu, and W. M. Liu, Vector solitons in two-component Bose-Einstein condensates with tunable interactions and harmonic potential, *Phys. Rev. A* **79**, 033630 (2009).
- [3] V. M. Pérez-García and J. B. Beitia, Symbiotic solitons in heteronuclear multicomponent Bose-Einstein condensates, *Phys. Rev. A* **72**, 033620 (2005).
- [4] S. K. Adhikari, Bright solitons in coupled defocusing NLS equation supported by coupling: Application to Bose-Einstein condensation, *Phys. Lett. A* **346**, 179 (2005).
- [5] H. E. Nistazakis, D. J. Frantzeskakis, P. G. Kevrekidis, B. A. Malomed, and R. Carretero-González, Bright-dark soliton complexes in spinor Bose-Einstein condensates, *Phys. Rev. A* **77**, 033612 (2008).
- [6] I. Danaila, M. A. Khamehchi, V. Gokhroo, P. Engels, and P. G. Kevrekidis, Vector dark-antidark solitary waves in multicomponent Bose-Einstein condensates, *Phys. Rev. A* **94**, 053617 (2016).
- [7] P. Öhberg and L. Santos, Dark Solitons in a Two-Component Bose-Einstein Condensate, *Phys. Rev. Lett.* **86**, 2918 (2001).
- [8] I. Morera, A. Muñoz Mateo, A. Polls, and B. Juliá-Díaz, Dark-dark-soliton dynamics in two density-coupled Bose-Einstein condensates, *Phys. Rev. A* **97**, 043621 (2018).
- [9] C. Becker, S. Stellmer, P. Soltan-Panahi, S. Dörscher, M. Baumert, E.-M. Richter, J. Kronjäger, K. Bongs, and K. Sengstock, Oscillations and interactions of dark and dark-bright solitons in Bose-Einstein condensates, *Nat. Phys.* **4**, 496 (2008).
- [10] T. Busch and J. R. Anglin, Dark-Bright Solitons in Inhomogeneous Bose-Einstein Condensates, *Phys. Rev. Lett.* **87**, 010401 (2001).
- [11] L. C. Zhao, Z. Y. Yang, and W. L. Yang, Solitons in nonlinear systems and eigen-states in quantum wells, *Chin. Phys. B* **28**, 010501 (2019).
- [12] L. D. Landau and E. M. Lifshitz, *Quantum Mechanics* (Nauka, Moscow, 1989).
- [13] L. C. Zhao, Beating effects of vector solitons in Bose-Einstein condensates, *Phys. Rev. E* **97**, 062201 (2018).
- [14] Y. Xu, Y. Zhang, and B. Wu, Bright solitons in spin-orbit-coupled Bose-Einstein condensates, *Phys. Rev. A* **87**, 013614 (2013).
- [15] V. Achilleos, D. J. Frantzeskakis, P. G. Kevrekidis, and D. E. Pelinovsky, Matter-Wave Bright Solitons in Spin-Orbit Coupled Bose-Einstein Condensates, *Phys. Rev. Lett.* **110**, 264101 (2013).
- [16] Y. C. Zhang, Z. W. Zhou, B. A. Malomed, and H. Pu, Stable Solitons in Three Dimensional Free Space without the Ground State: Self-Trapped Bose-Einstein Condensates with Spin-Orbit Coupling, *Phys. Rev. Lett.* **115**, 253902 (2015).
- [17] S. Gautam and S. K. Adhikari, Three-dimensional vortex-bright solitons in a spin-orbit-coupled spin-1 condensate, *Phys. Rev. A* **97**, 013629 (2018).
- [18] D. Edler, C. Mishra, F. Wächtler, R. Nath, S. Sinha, and L. Santos, Quantum Fluctuations in Quasi-One-Dimensional Dipolar Bose-Einstein Condensates, *Phys. Rev. Lett.* **119**, 050403 (2017).
- [19] P. Cheiney, C. R. Cabrera, J. Sanz, B. Naylor, L. Tanzi, and L. Tarruell, Bright Soliton to Quantum Droplet Transition in a Mixture of Bose-Einstein Condensates, *Phys. Rev. Lett.* **120**, 135301 (2018).
- [20] H. Kadau, M. Schmitt, M. Wenzel, C. Wink, T. Maier, I. Ferrier-Barbut, and T. Pfau, Observing the Rosensweig instability of a quantum ferrofluid, *Nature (London)* **530**, 194 (2016).
- [21] C. R. Cabrera, L. Tanzi, J. Sanz, B. Naylor, P. Thomas, P. Cheiney, and L. Tarruell, Quantum liquid droplets in a mixture of Bose-Einstein condensates, *Science* **359**, 301 (2018).
- [22] N. B. Jørgensen, G. M. Bruun, and J. J. Arlt, Dilute Fluid Governed by Quantum Fluctuations, *Phys. Rev. Lett.* **121**, 173403 (2018).
- [23] S. Gautam and S. K. Adhikari, Self-trapped quantum balls in binary Bose-Einstein condensates, *J. Phys. B: At., Mol. Opt. Phys.* **52**, 055302 (2019).
- [24] B. Gertjerenken, T. P. Billam, C. L. Blackley, C. R. Le Sueur, L. Khaykovich, S. L. Cornish, and C. Weiss, Generating Mesoscopic Bell States via Collisions of Distinguishable Quantum Bright Solitons, *Phys. Rev. Lett.* **111**, 100406 (2013).
- [25] L. C. Zhao and J. Liu, Localized nonlinear waves in a two-mode nonlinear fiber, *J. Opt. Soc. Am. B* **29**, 3119 (2012).
- [26] P. G. Kevrekidis and D. J. Frantzeskakis, Solitons in coupled nonlinear Schrödinger models: A survey of recent developments, *Rev. Phys.* **1**, 140 (2016).
- [27] G. P. Agrawal, *Nonlinear Fiber Optics*, 4th ed. (Academic, San Diego, 2007).
- [28] K. Nithyanandan, R. Vasantha Jayakantha Raja, K. Porsezian, and B. Kalithasan, Modulational instability with higher-order dispersion and walk-off in Kerr media with cross-phase modulation, *Phys. Rev. A* **86**, 023827 (2012).
- [29] V. B. Matveev and M. A. Salle, *Darboux Transformation and Solitons* (Springer-Verlag, Berlin, 1991).
- [30] E. V. Doktorov and S. B. Leble, *A Dressing Method in Mathematical Physics* (Springer-Verlag, Berlin, 2007).

- [31] B. L. Guo, L. Ling, and Q. P. Liu, Nonlinear Schrödinger equation: Generalized Darboux transformation and rogue wave solutions, *Phys. Rev. E* **85**, 026607 (2012).
- [32] L. Ling, L. C. Zhao, and B. Guo, Darboux transformation and multi-dark soliton for N -component nonlinear Schrödinger equations, *Nonlinearity* **28**, 3243 (2015).
- [33] R. Hirota, *The Direct Method in Soliton Theory* (Cambridge University, Cambridge, England, 2004).
- [34] T. Kanna and M. Lakshmanan, Exact Soliton Solutions, Shape Changing Collisions, and Partially Coherent Solitons in Coupled Nonlinear Schrödinger Equations, *Phys. Rev. Lett.* **86**, 5043 (2001).
- [35] Q. H. Park and H. J. Shin, Systematic construction of multicomponent optical solitons, *Phys. Rev. E* **61**, 3093 (2000).
- [36] B. F. Feng, General N -soliton solution to a vector nonlinear Schrödinger equation, *J. Phys. A* **47**, 355203 (2014).
- [37] Y. J. Zhang and Y. Cheng, Solutions for the vector k -constrained KP hierarchy, *J. Math. Phys.* **35**, 5869 (1994).
- [38] B. Dubrovin, T. Malanyuk, I. Krichever, and V. Makhankov, Exact solutions of the time-dependent Schrödinger equation with self-consistent potential, *Sov. J. Part. Nucl.* **19**, 252 (1988).
- [39] L. C. Zhao and S. L. He, Matter wave solitons in coupled system with external potentials, *Phys. Lett. A* **375**, 3017 (2011).
- [40] R. Radhakrishnan and M. Lakshmanan, Bright and dark soliton solutions to coupled nonlinear Schrödinger equations, *J. Phys. A: Math. Gen.* **28**, 2683 (1995).
- [41] N. Akhmediev and A. Ankiewicz, Multi-soliton complexes, *Chaos* **10**, 600 (2000).
- [42] I. V. Barashenkov and S. R. Woodford, Complexes of stationary domain walls in the resonantly forced Ginsburg-Landau equation, *Phys. Rev. E* **71**, 026613 (2005).
- [43] I. V. Barashenkov and S. R. Woodford, Interactions of parametrically driven dark solitons. II. Néel-Bloch interactions, *Phys. Rev. E* **75**, 026605 (2007).
- [44] S. Stalin, R. Ramakrishnan, M. Senthilvelan, and M. Lakshmanan, Nondegenerate Solitons in Manakov System, *Phys. Rev. Lett.* **122**, 043901 (2019).
- [45] M. Mitchell, M. Segev, and D. N. Christodoulides, Observation of Multihump Multimode Solitons, *Phys. Rev. Lett.* **80**, 4657 (1998).
- [46] E. A. Ostrovskaya, Y. S. Kivshar, D. V. Skryabin, and W. J. Firth, Stability of Multihump Optical Solitons, *Phys. Rev. Lett.* **83**, 296 (1999).
- [47] M. Haelterman and A. Sheppard, Bifurcation phenomena and multiple soliton-bound states in isotropic Kerr media, *Phys. Rev. E* **49**, 3376 (1994).
- [48] N. Akhmediev, W. Krolikowski, and A. W. Snyder, Partially Coherent Solitons of Variable Shape, *Phys. Rev. Lett.* **81**, 4632 (1998); A. Ankiewicz, W. Krolikowski, and N. N. Akhmediev, Partially coherent solitons of variable shape in a slow Kerr-like medium: Exact solutions, *Phys. Rev. E* **59**, 6079 (1999).
- [49] L. C. Zhao, L. Ling, Z. Y. Yang, and J. Liu, Properties of the temporal-spatial interference pattern during soliton interaction, *Nonlinear Dyn.* **83**, 659 (2016).
- [50] T. M. Berano, V. Gokroo, M. A. Khamehchi, J. D. Abroise, D. J. Frantzeskakis, P. Engels, and P. G. Kevrekidis, Three-Component Soliton States in Spinor $F = 1$ Bose-Einstein Condensate, *Phys. Rev. Lett.* **120**, 063202 (2018).
- [51] C. Hamner, J. J. Chang, and P. Engels, Generation of Dark-Bright Soliton Trains in Superfluid-Superfluid Counterflow, *Phys. Rev. Lett.* **106**, 065302 (2011).
- [52] M. A. Hoefer, J. J. Chang, C. Hamner, and P. Engels, Dark-dark solitons and modulational instability in miscible two-component Bose-Einstein condensates, *Phys. Rev. A* **84**, 041605(R) (2011).
- [53] T. P. Billam, S. L. Cornish, and S. A. Gardiner, Realizing bright-matter-wave-soliton collisions with controlled relative phase, *Phys. Rev. A* **83**, 041602(R) (2011).
- [54] A. L. Marchant, T. P. Billam, T. P. Wiles, M. M. H. Yu, S. A. Gardiner, and S. L. Cornish, Controlled formation and reflection of a bright solitary matter-wave, *Nat. Commun.* **4**, 1865 (2013).
- [55] P. Medley, M. A. Minar, N. C. Cizek, D. Berryrieser, and M. A. Kasevich, Evaporative Production of Bright Atomic Solitons, *Phys. Rev. Lett.* **112**, 060401 (2014).
- [56] J. H. V. Nguyen, P. Dyke, D. Luo, B. A. Malomed, and R. G. Hulet, Collisions of matter-wave solitons, *Nat. Phys.* **10**, 918 (2014).